Investigation of the reactivity of $AlCl_3$ and $CoCl_2$ toward molten alkali-metal nitrates in order to synthesize $CoAl_2O_4$

N. Ouahdi, S. Guillemet, J.J. Demai, B. Durand, L. Er Rakho, R. Moussa and A. Samdi

Centre Interuniversitaire de Recherche et d'Ingénierie des Matériaux/Laboratoire de Chimie des Matériaux Inorganiques et Energétiques, CNRS UMR 5085, Université Paul Sabatier Bât 2R1, 118 route de Narbonne, 31062 Toulouse cedex 04, France
Equipe Microstructure et Physico-chimie des Matériaux, UFR Physico-chimie des Matériaux (C53/97), Faculté des Sciences Aïn Chock, Université Hassan II, B.P 5366 Mâarif, Casablanca, Morocco

Abstract

Cobalt aluminate $CoAl_2O_4$ powder, constituted of nano-sized crystallites, is prepared, involving the reactivity of $AlCl_3$ and $CoCl_2$ with molten alkali-metal nitrates. The reaction at 450 °C for 2 h leads to a mixture of spinel oxide Co_3O_4 and amorphous γ-Al_2O_3. It is transformed into the spinel oxide $CoAl_2O_4$ by heating at 1000 °C. The powders are mainly characterized by XRD, FTIR, ICP, electron microscopy and diffraction, X-EDS and diffuse reflection. Their properties are compared to those of powders obtained by solid state reactions of a mechanical mixture of chlorides or oxides submitted to the same thermal treatment.

Keywords: Cobalt aluminate; Spinel structure; Reactions in molten salts; Nanomaterials; X-ray techniques; Electron microscopy

1. Introduction

Most of the ceramic dyeing materials are transition metal oxides crystallizing in the spinel structure which gives high thermal stability and chemical resistance. It is characterized by a simultaneous occupation of tetrahedral and octahedral positions by metals in a FCC oxygen frame. Among them, cobalt aluminate $CoAl_2O_4$ is well known as Thenard's blue. It exhibits the normal spinel structure and is widely used in ceramic, glass, paint industry and for color TV tubes as contrast-enhancing luminescent pigment [1] and [2]. It is also an important material for heterogeneous catalysis, as example for the CO_2 reforming of methane [3].

The most general method to prepare spinel oxides involves solid state reaction of mechanically mixed parent oxides. However, for complete reaction, a temperature of at least 1300 °C has to be maintained for long time periods [4] and [5]. Recently, $CoAl_2O_4$ has been prepared by various solution chemical synthesis techniques: sol–gel process [6], [7], [8], [9] and [10], coprecipitation [11] and [12], hydrothermal synthesis [13], polymeric precursor method [14] and [15] and polyol method [16].

In molten state, the oxo-salts of alkali-metals (nitrites, nitrates, carbonates, sulfates, etc.) are ionic liquids characterized by dissolvent properties stronger than those of aqueous media because of their higher melting points [17]. Thus, they allow to perform chemical reactions producing fine oxide powders with specific properties [18] and [19]. In the reactions of transition metal salts with molten media constituted of alkali-metal and oxo-anion salts, the oxo-anion is involved as a Lux–Flood base, i.e. a donor of oxide anions O^{2-}, whereas the transition metal cation reacts as a Lux–Flood acid, i.e. an acceptor of O^{2-} anions [20]. Thus various simple or mixed oxides, characterized by high specific surface area and excellent chemical composition homogeneity, have been prepared by reaction, at 450 °C for a few hours, of transition metal salts in molten alkali-metal nitrates: x mol% Y_2O_3–ZrO_2 ($0 \leq x \leq 8$) [21], Al_2O_3–ZrO_2 dispersions [22], TiO_2 anatase [23], CeO_2 [24], 3 mol% Y_2O_3–HfO_2 [25], $PbTiO_3$ [26].

Such reactions have never been used for the preparation of $CoAl_2O_4$. The only informations found in the literature concern thermogravimetric studies of the reactivity of cobalt chloride in molten nitrate eutectic. According to Frouzanfar and Kerridge [27], anhydrous $CoCl_2$ reacts with molten $LiNO_3$–KNO_3 eutectic (M.P. 125 °C) to form the mixed valence oxide Co_3O_4 via reaction (1). The reaction occurs with a maximum rate at about 380 °C and is over below 500 °C. Replacing $LiNO_3$–KNO_3 by $NaNO_3$–KNO_3 eutectic (M.P. 225 °C), Singh and Pandey [28] have noticed that the reaction occurs in the same temperature range (beginning at 280 °C, maximum rate at 380 °C, end of the reaction below 500 °C) and leads also to Co_3O_4, but they consider that cobalt chloride is first transformed into cobalt nitrate via reaction (2) and then decomposes into Co_3O_4 via reaction (3). The authors conclude that both reactions proceed by diffusion in solid state.

$$3CoCl_2+7NO_3^- \rightarrow Co_3O_4+NO_2^-+6NO_2+3/2\ O_2+6Cl^- \quad (1)$$

$$CoCl_2+NaNO_3+KNO_3 \rightarrow Co(NO_3)_2+NaCl+KCl \quad (2)$$

$$3Co(NO_3)_2 \rightarrow Co_3O_4+6NO_2+O_2 \quad (3)$$

Concerning the stability of aluminium trichloride, Topol et al. [29] have related that, in molten

$NaNO_3$–KNO_3 eutectic, aluminium nitrate evolves a brownish gas at 285 °C, whereas Kerridge and Shakir [30], after a more thorough study of the reaction of aluminium chloride with molten $LiNO_3$–KNO_3 eutectic have concluded that α-Al_2O_3 is formed by a two-step reaction with two maximum rates at respectively 200 and 280 °C, via Eq. (4). The double maximum could indicate partial stabilization of aluminium cations by formation of $AlCl_4^-$ anions.

$$2AlCl_3+6NO_3^-\rightarrow Al_2O_3+6Cl^-+6NO_2+3/2O_2 \quad (4)$$

The present paper deals with the investigation of the reactivity of $AlCl_3$ and $CoCl_2$ in molten alkali-metal nitrates in order to prepare $CoAl_2O_4$ and with the comparison of the properties of the powders obtained with those of powders synthesized by solid state reactions.

2. Experimental

2.1. Chemical reagents

The aluminium and cobalt sources were either reagent grade chlorides $AlCl_3{\cdot}6H_2O$ (Fluka) and $CoCl_2{\cdot}6H_2O$ (Prolabo) or reagent grade oxides γ-Al_2O_3 (Aldrich) and Co_3O_4 prepared by calcination of $CoCl_2{\cdot}6H_2O$ at 800 °C. The cobalt oxide formed was identified by XRD. The weight loss measured by thermogravimetric analysis agrees with that calculated for the transformation of $CoCl_2{\cdot}6H_2O$ into Co_3O_4. The molten medium was the equimolar mixture of reagent grade $NaNO_3$ and KNO_3 (Aldrich) corresponding to the lowest melting point (225 °C) in the binary phase diagram.

All the salts were oven-dried overnight (150 °C for $CoCl_2{\cdot}6H_2O$, 110 °C for $AlCl_3{\cdot}6H_2O$ and the alkali-metal nitrates), then cooled at room temperature and kept in a desiccator before use.

2.2. Synthesis procedure

2.2.1. Molten salts method

Taking into account previous results concerning the synthesis of zirconia by reaction of zirconium oxychloride with molten alkali-metal nitrates [21] and [27], the synthesis of $CoAl_2O_4$ was postulated to occur according to Eq. (5) in which the reduction of NO_3^- into NO_2 is balanced by the oxidation of Cl^- into chlorine.

$$CoCl_2+2AlCl_3+4NO_3^-\rightarrow CoAl_2O_4+4NO_2+2Cl_2+4Cl^- \quad (5)$$

The reaction medium contained a significant excess of alkali-metal nitrates with respect to the stoichiometry of Eq. (5), so as to get a complete reaction within 2 h. The involved molar proportions were about 10 ($NaNO_3$–KNO_3) for 1$CoCl_2$ and 2$AlCl_3$, i.e. five times the stoichiometric molar ratio. It was formed by quickly blending a mixture $CoCl_2$+2$AlCl_3$ and a mixture $NaNO_3$–KNO_3 prepared separately and then poured in the reaction tube of a vertical Pyrex reactor. Some thermogravimetric preliminary experiments were carried out so as to check

separately the reactivity of $CoCl_2$ and that of $AlCl_3$ with molten $NaNO_3$–KNO_3 eutectic. For $CoCl_2$, results comparable to those of literature [27], [28] and [29] were obtained, i.e. complete formation of Co_3O_4 at a temperature lower than 500 °C. For $AlCl_3$, we did not observe the formation of α-Al_2O_3, but that of a low-crystallinity γ-Al_2O_3 also below 500 °C. Consequently, for the investigation of the reaction of both precursors in the same molten bath, the heating rate and the reaction temperature were set at respectively 150 °C h^{-1} and 450 °C, holding a dwell for 2 h. The cooling rate was not controlled.

During the thermal treatment, the exhausted gases were swept away by an air flow and bubbled inside a sodium hydroxide solution so as to eliminate NO_2 and Cl_2. After cooling at room temperature, the insoluble oxide powder formed was recovered by filtration after washing away the excess of nitrates and alkali-metal chlorides, by dissolution in water. Finally, the oxide powder was dried at 120 °C overnight. The sample was named MS450.

Then the oxide powder MS450 was heated at temperatures θ, in the range 800–1200 °C at a rate of 180 °C h^{-1} without maintaining a dwell, giving samples referenced MSθ.

2.2.2. Solid–solid reactions

Diffusion reactions in solid state were performed starting from intimate mixtures of either Co_3O_4 and Al_2O_3 or $CoCl_2{\cdot}6H_2O$ and $AlCl_3{\cdot}6H_2O$ with, in both cases, a molar ratio Al/Co fixed at 2. The thermal treatments were carried out exactly under the same conditions that the heating of sample MS450, i.e. same temperature and heating rate, no dwell, use of the same muffle furnace. The samples were referenced OXθ and CLθ (θ is the temperature, OX is oxide precursors and CL is chloride precursors).

2.3. Reactivity and powder characterization

The occurrence of chemical reactions between the transition metal precursors and the molten alkali-metal nitrates was evidenced by a brown red NO_2 release.

The obtained oxide powders were characterized by X-ray diffraction (DRX, Siemens D501 diffractometer for powders, $\lambda_{CuK\alpha}$=1.5418 Å), Fourier transformed infrared spectroscopy (FTIR, Perkin Elmer 1760), scanning and transition electron microscopies (SEM, Jeol JSM 6400 provided with energy dispersion X-EDS; TEM, Jeol 2010), specific surface area measurements by nitrogen adsorption (Micrometrics Accusorb 2100 E, defined by BET method), size distribution analysis by laser deviation (Malvern Mastersizer 2000S), chemical analysis by inductively coupled plasma spectroscopy (ICP Jobin Yvon 24) and themogravimetric and differential thermic analyses (TGA–DTA, Setaram TAG 24 thermoanalyser).

The diffuse reflection was measured with a lambda 19 Perkin Elmer spectrometer equipped with an integrating sphere and monochromators for incoming as well as reflected light. Spectra were recorded in the range 200–800 nm.

3. Results

3.1. Reactions in molten salts

3.1.1. Characterization of sample MS450

The XRD pattern of the black powder obtained exhibits a family of sharp peaks characteristic of a spinel phase, undoubtedly identified as Co_3O_4, and several broad signals all attributed, in agreement with Ref. [32], to low-crystallinity γ-Al_2O_3 (Fig. 1a). The differentiation between the spinel phases Co_3O_4 and $CoAl_2O_4$ is obtained from the relative intensities of peaks (111), (222) and (331). Indeed (Table 1), the intensities of peaks (111) and (222) are significantly stronger in Co_3O_4 than in $CoAl_2O_4$, whereas the one of peak (331) is a little stronger in $CoAl_2O_4$ than in Co_3O_4.

Fig. 1. XRD pattern of samples MS450 (a), MS800 (b), MS1000 (c) and MS1200 (d) —★α-Al_2O_3, ▼ γ-Al_2O_3, ● $CoAl_2O_4$ and Co_3O_4.

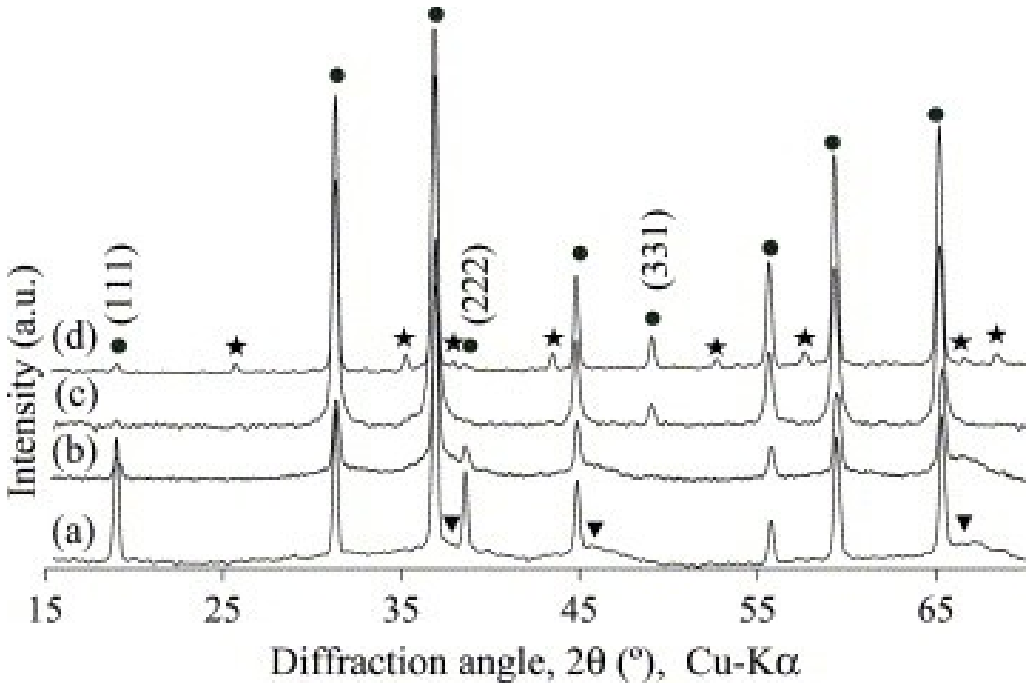

Table 1.

Comparison of the localization ($\lambda_{CuK\alpha}$=1.5418 Å, 2θ (degree)) and relative intensities of XRD peaks (111), (222) and (331) in Co_3O_4 (JCPDS file no. 80-1535) and $CoAl_2O_4$ (JCPDS file no. 82-2252)

	hkl	**111**	**222**	**331**
$CoAl_2O_4$	2θ, I/I_0	18.95, 5	38.436, <1	48.94, 4

	hkl	111	222	331
Co_3O_4		18.89, 54	38.326, 27	48.79, <1

The FTIR spectrum, in the wave number range 400–1000 cm^{-1}, reveals two narrow bands centered around 584 and 668 cm^{-1}, a shoulder at 650 cm^{-1} and two large bands, one around 540 cm^{-1} and the other spread from 700 to 900 cm^{-1} (Fig. 2a, Table 2). The three first signals are characteristic of Co_3O_4 (588, 655 and 670 cm^{-1} according to Ref. [31]). The large bands indicate the presence of γ-Al_2O_3 (500–850 cm^{-1} according to Ref. [32]).

Fig. 2. FTIR spectrum of samples MS450 (a), MS800 (b), MS1000 (c) and MS1200 (d).

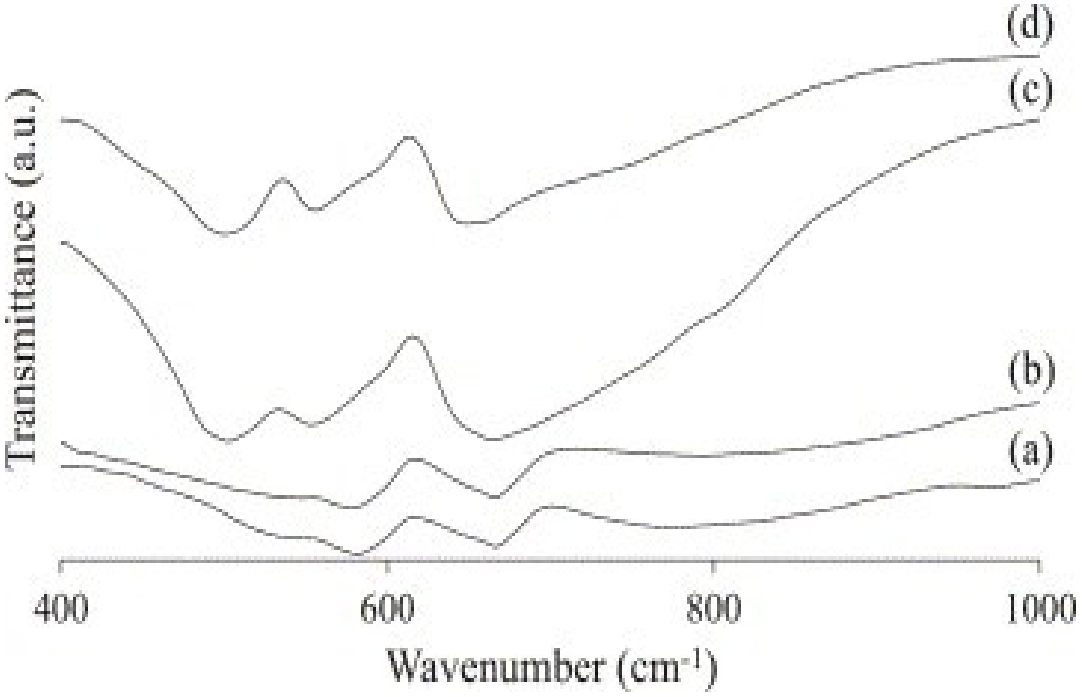

Table 2.

Attribution of bands and shoulders in the FTIR spectrum of the powders obtained (wave number in cm^{-1})

Sample	Co_3O_4	$CoAl_2O_4$	γ-Al_2O_3	α-Al_2O_3
MS450	584, 650, 668		540, 700–900	
MS800	584, 650, 668		540, 700–900	
MS1000		500, 555, 660		640
MS1200		500, 555, 660		450, 590, 640
CL800	570, 650, 667		540, 700–900	

Sample	Co_3O_4	$CoAl_2O_4$	γ-Al_2O_3	α-Al_2O_3
CL1000	560, 650, 667	500, 560, 663		
CL1200	560, 650, 667	500, 560, 663		
OX800	580, 650, 666		540, 700–900	590
OX1000	584, 650, 666	500, 557, 660		640, 590
OX1200	584, 650, 666	500, 557, 660		444, 590, 640

The examination by scanning electron microscopy, electron diffraction and energy dispersion of X-rays (X-EDS) shows the presence of two kinds of particles in the powder (Fig. 3). The first one, constituted of crystallized octahedral particles rich in cobalt and very poor in aluminium, is identified as Co_3O_4. The second one made of amorphous particles with no definite shape, rich in aluminium and very poor in cobalt, is identified as low-crystallinity γ-Al_2O_3. For both kinds of particles, the presence of Ag peaks in the fluorescence patterns is due to the metallization of the powder before examination.

Fig. 3. Electron micrographs (a, b), electron diffraction patterns (c, d) and X-EDS patterns (e, f) of sample MS450—(a, c, e) area rich in Al, (b, d, f) area rich in Co.

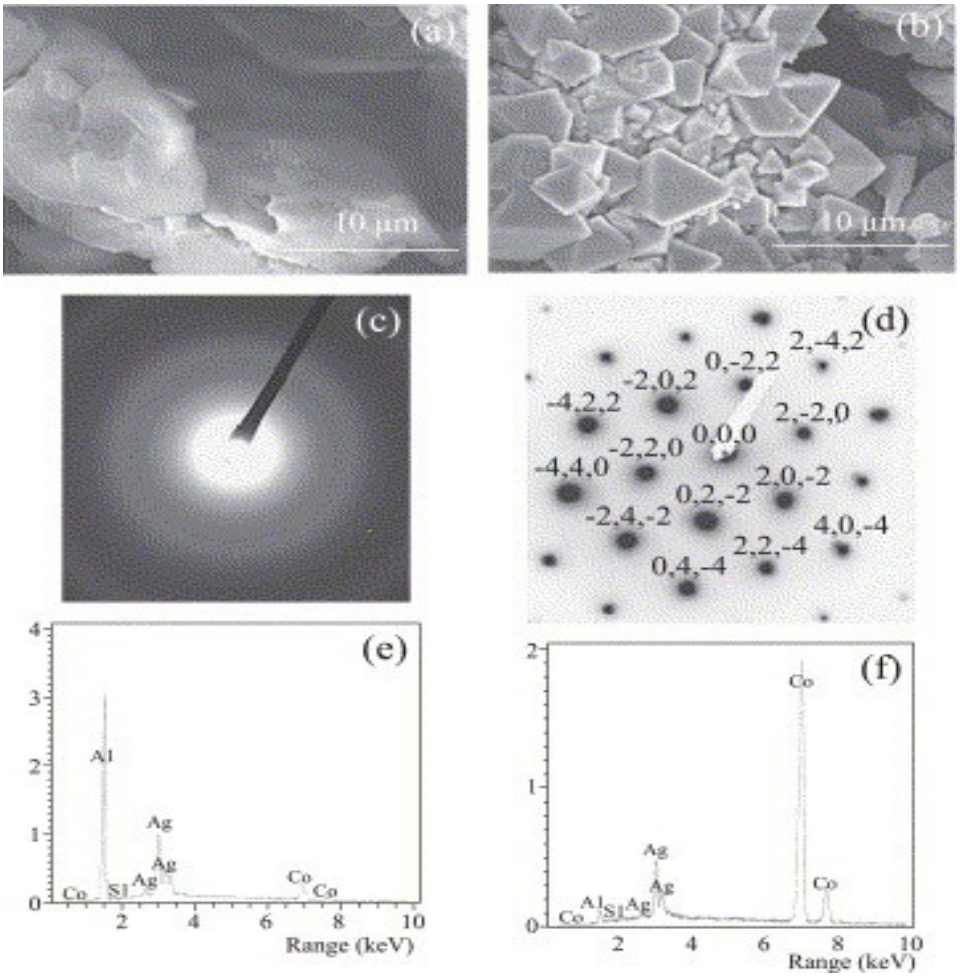

The coupled DTA–TGA analysis (Fig. 4) shows a weight loss occurring in three steps involving three endothermic effects. The first one, about 13 wt.%, occurring in the range 50–200 °C with maximum rate at 100 °C, is attributed to the release of water physisorbed on both kinds of particles. The second one, about 5 wt.%, occurring in the range 200–600 °C with maximum rate at about 400 °C is attributed to the evolution of water chemisorbed. The third one (2.5 wt.%), occurring on a narrower temperature range with maximum rate at about 900 °C is attributed to the reduction of Co(III) into Co (II). The exothermic effect at about 1120 °C is attributed to the crystallization of γ-Al_2O_3 into α-Al_2O_3.

Fig. 4. TGA–DTA curves of sample MS450 (heating rate: 3 °C min^{-1}).

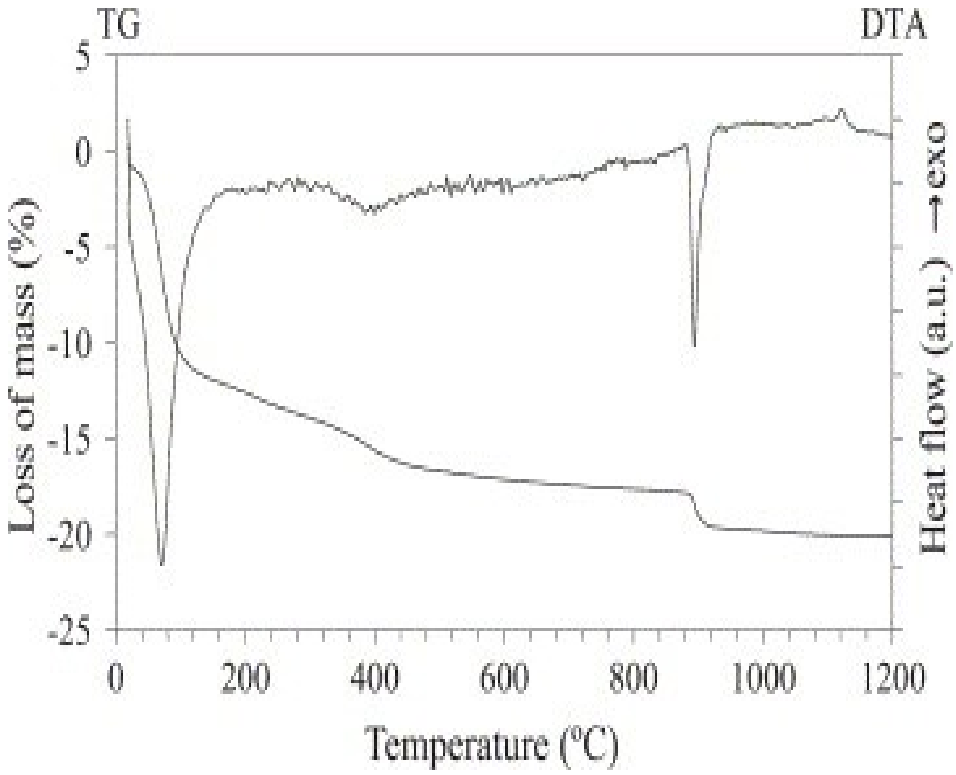

The powder MS450 exhibits a high specific surface area close to 250 m^2 g^{-1}. It is mainly due to the presence of low-crystallinity γ-Al_2O_3.

3.1.2. Characterization of samples MS800, MS1000 and MS1200

The XRD patterns of the heated powders (Fig. 1b,c,d) show the progressive formation of $CoAl_2O_4$ by reaction between Co_3O_4 and γ-Al_2O_3. Sample MS800 differs from MS450 by a significant decrease of the intensity of all peaks, particularly that of peaks (111) and (222) characteristic of the presence of Co_3O_4. The low-crystallinity γ-Al_2O_3 is still present. The peak (331), characteristic of $CoAl_2O_4$ appears in the pattern of MS1000, whereas the peaks (111) and (222) and the broad signals of the amorphous phase are no more visible. The pattern of MS1200 unveils an improvement of the crystallinity of $CoAl_2O_4$ and the presence of very little proportion of α-Al_2O_3.

A similar evolution is revealed by the FTIR spectra of the heated powders (Fig. 2b,c,d, Table 2). For sample MS800, the bands of Co_3O_4 are located at 584, 650 and 668 cm^{-1} and the

intensity of bands of γ-Al_2O_3 are lower than in MS450. The spectrum of sample MS1000 is characterized by the disappearance of the band of Co_3O_4 at 584 cm^{-1} and the appearance of two bands at 550 and 555 cm^{-1} typical of the presence of $CoAl_2O_4$.The shoulder at 640 cm^{-1} may indicate the presence of a very small proportion of α-Al_2O_3 not discernable par XRD. In addition to the bands of $CoAl_2O_4$, the spectrum of MS1200 exhibits bands at 450, 590 and 640 cm^{-1} that corroborate the formation of α-Al_2O_3 already identified by XRD.

The TEM micrographs of sample MS1000 (Fig. 5) show submicronic agglomerates constituted of nanosized crystallites (20–40 nm). The characterization by energy dispersion of X-rays (X-EDS) indicates a molar ratio Al/Co of 1.99 whatever the examined area and the rings of the electron diffraction pattern correspond to $CoAl_2O_4$.

Fig. 5. Electron diffraction pattern (a) and electron micrograph (b) of sample MS1000.

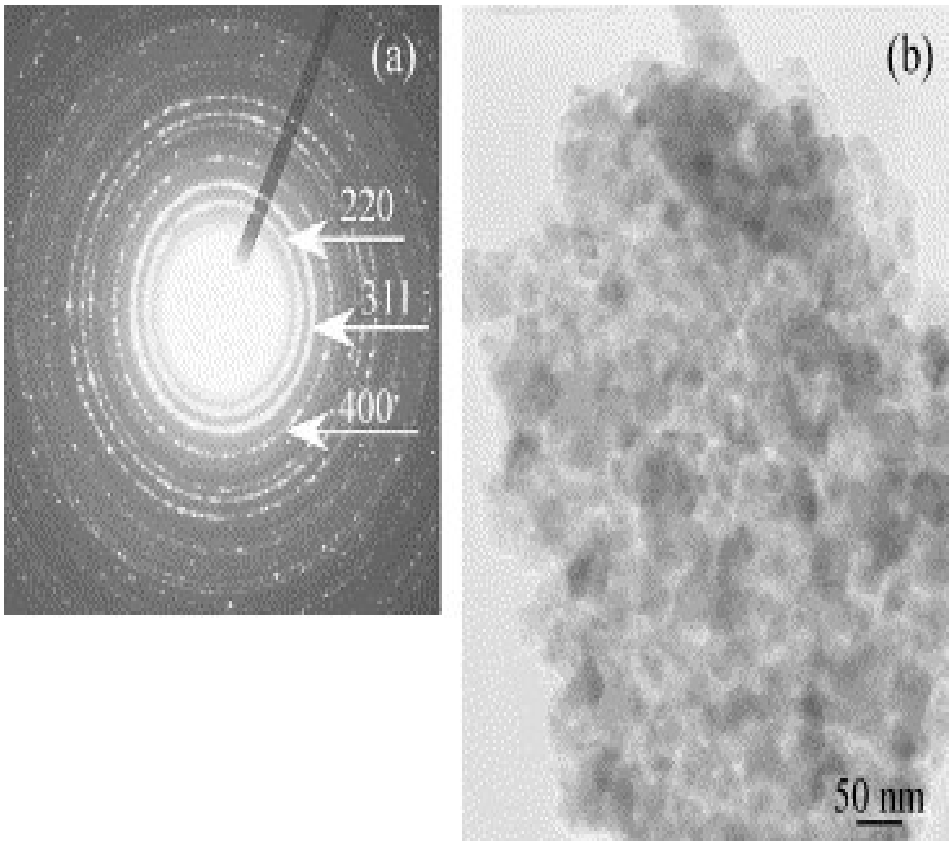

In the powder MS1000, the size of the agglomerates is spread from a few μm to 100 μm with a maximum at 30 μm (Fig. 6). The UV–Visible spectrum of samples MS1000 and MS1200 exhibits a minimum of absorption near 500 nm and a absorption maximum from about 540 to 640 nm (Fig. 7). These values are in agreement with previous results [12] and [16].

Fig. 6. Particle size distribution of sample MS1000.

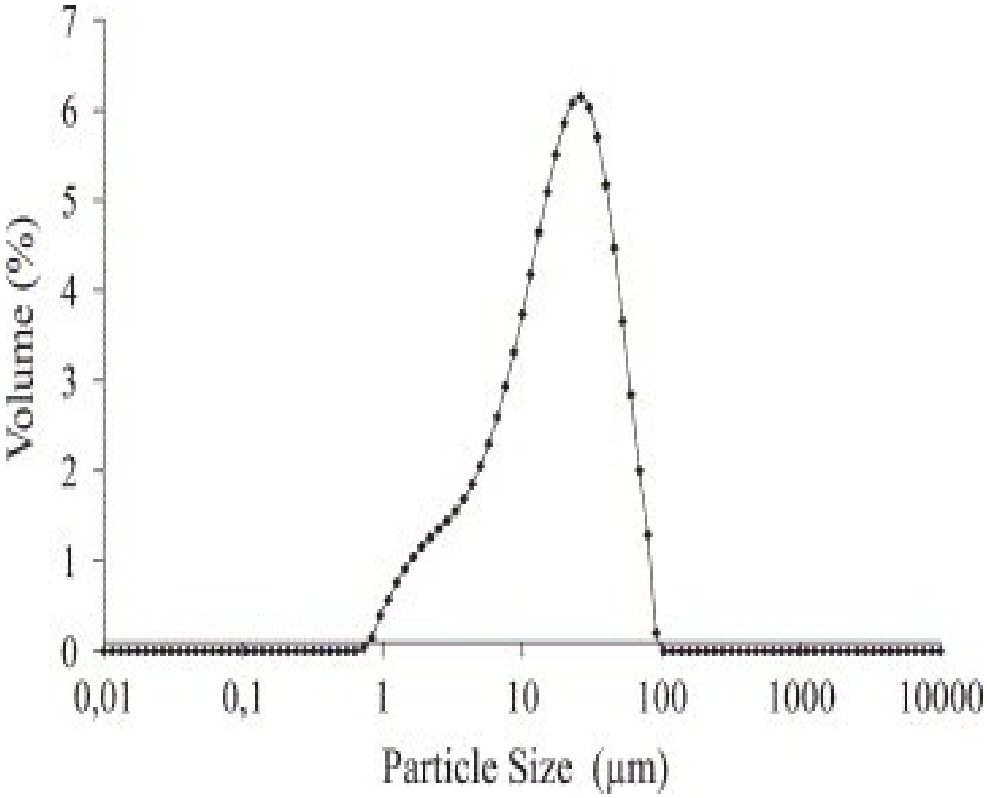

Fig. 7. UV–Visible spectrum of samples MS1000 (a) and MS1200 (b).

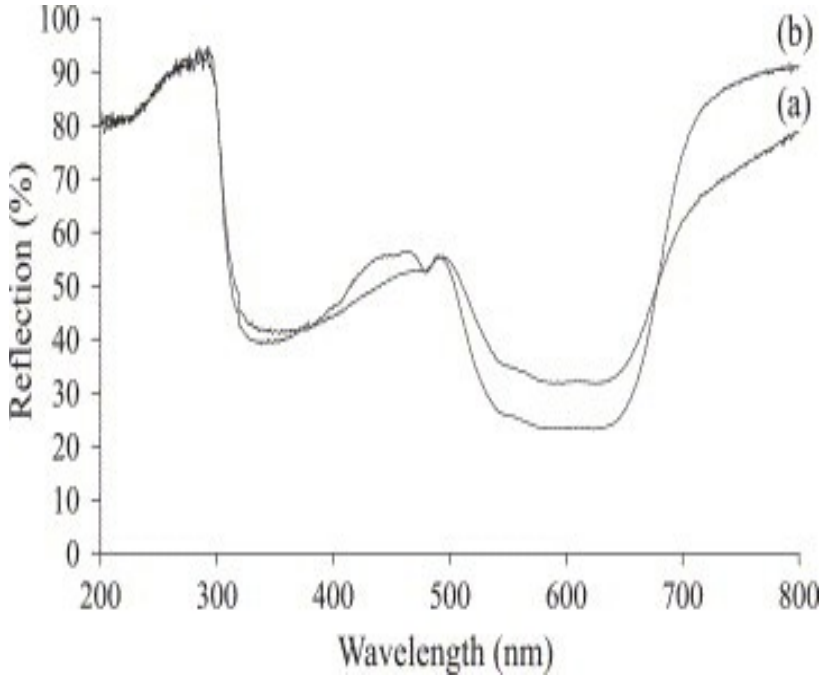

The specific surface area is respectively 3 and 29 $m^2\ g^{-1}$ for samples MS1200 and MS1000.

3.2. Solid–solid reactions

3.2.1. Thermal treatment of the chloride mixture

The XRD patterns of samples CL800, CL1000 and CL1200 (Fig. 8) are very similar. The peak (111) of the spinel phase at 2θ=18.9°, characteristic of Co_3O_4, is present in the three diffraction diagrams and the peak (331) at 2θ=48.9° indicating the formation of $CoAl_2O_4$ is clearly identified in the diagram of samples CL1000 and CL1200. The presence of α-Al_2O_3 is not detected.

Fig. 8. XRD pattern of samples CL800 (a), CL1000 (b) and CL1200 (c).

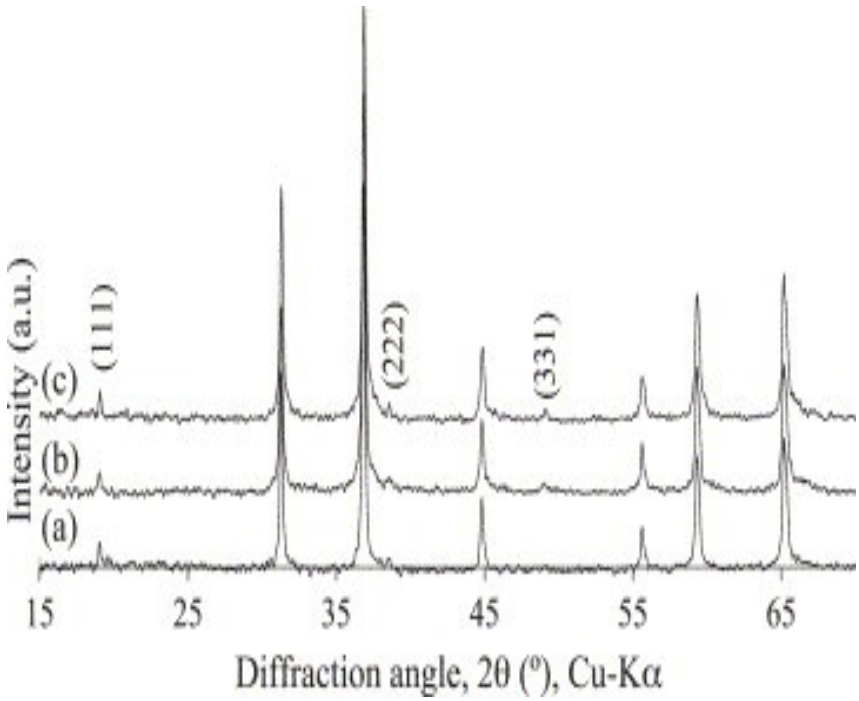

The FTIR spectrum of sample CL800 (Fig. 9a, Table 2) exhibits similarities with the one of sample MS800 and reveals the presence of a mixture of Co_3O_4 (570, 650 and 667 cm^{-1}) and γ-Al_2O_3 (540, 700–900 cm^{-1}). The FTIR spectra of samples CL1000 and CL1200 (Fig. 9b,c, Table 2) are quite identical and identify mixtures of Co_3O_4 (560, 650, 667 cm^{-1}) and $CoAl_2O_4$ (500, 560, 663 cm^{-1}). The band of alumina at 540 cm^{-1} is no more visible and the large one at 700–900 cm^{-1} is strongly softened. As the heating temperature increases, the powder color changes from black (CL800) to dark blue (CL1000, CL1200).

Fig. 9. FTIR spectrum of samples CL800 (a), CL1000 (b) and CL1200 (c).

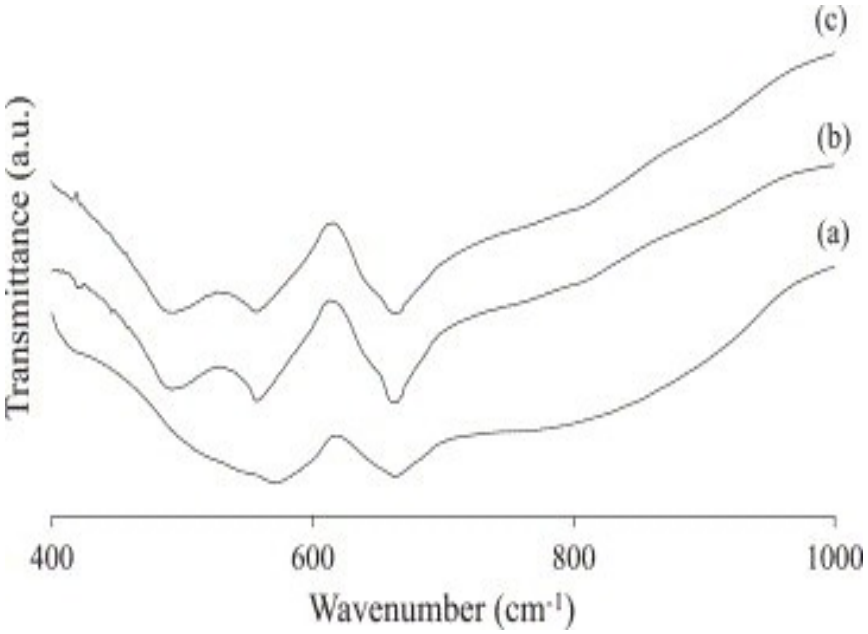

From XRD and FTIR analyses, it is concluded that during the calcination of a mixture of cobalt and aluminium chlorides, the formation of $CoAl_2O_4$ begins to occur above 800 °C and is not finished at 1200 °C. Moreover, the determination of the molar ratio Al/Co by X-EDS reveals great heterogeneities of the chemical composition, that ratio varying in the range 1.1–4.3 according to the investigated area.

3.2.2. Thermal treatment of mixtures of oxides

The XRD pattern of sample OX800 (Fig. 10a) reveals the presence of the starting materials, well crystallized Co_3O_4 and amorphous γ-Al_2O_3, but also that of a small proportions of α-Al_2O_3 (strongest peak at 2θ=35.12°). The raise of the calcination temperature at 1000 and then 1200 °C (Fig. 10b,c) decreases the proportion of Co_3O_4 (decrease of the intensity of peaks (111) and (222)) which is partially transformed into $CoAl_2O_4$ from 1000 °C (appearance and then increase of the intensity of the peak (331), change of the color from gray to blue). The main difference with sample obtained from chlorides is the presence of a significant proportion of α-Al_2O_3 in sample OX1200.

Fig. 10. XRD pattern of samples OX800 (a), OX1000 (b) and OX1200 (c)—★ αAl_2O_3, ● $CoAl_2O_4$ and Co_3O_4.

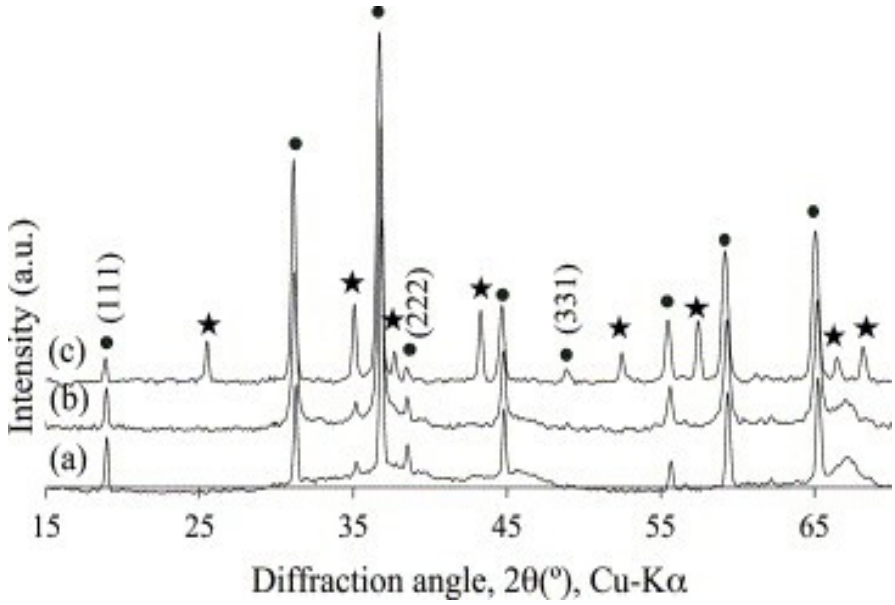

Here again, the FTIR spectrum of sample OX800 shows the presence of a mixture of Co_3O_4 and γ-Al_2O_3 and the one of sample OX1000 the formation of a mixture Co_3O_4 and $CoAl_2O_4$ (Fig. 11a,b, Table 2). In both cases, a shoulder at about 590 cm^{-1} corroborates the presence of α-Al_2O_3 detected by XRD. The spectrum of sample OX1200 differs from that of samples CL1000 (Fig. 11c, Table 2) by the strong intensity of bands of α-Al_2O_3 at 444, 590 and 640 cm^{-1}.

Fig. 11. FTIR spectrum of samples OX800 (a), OX1000 (b) and OX1200 (c).

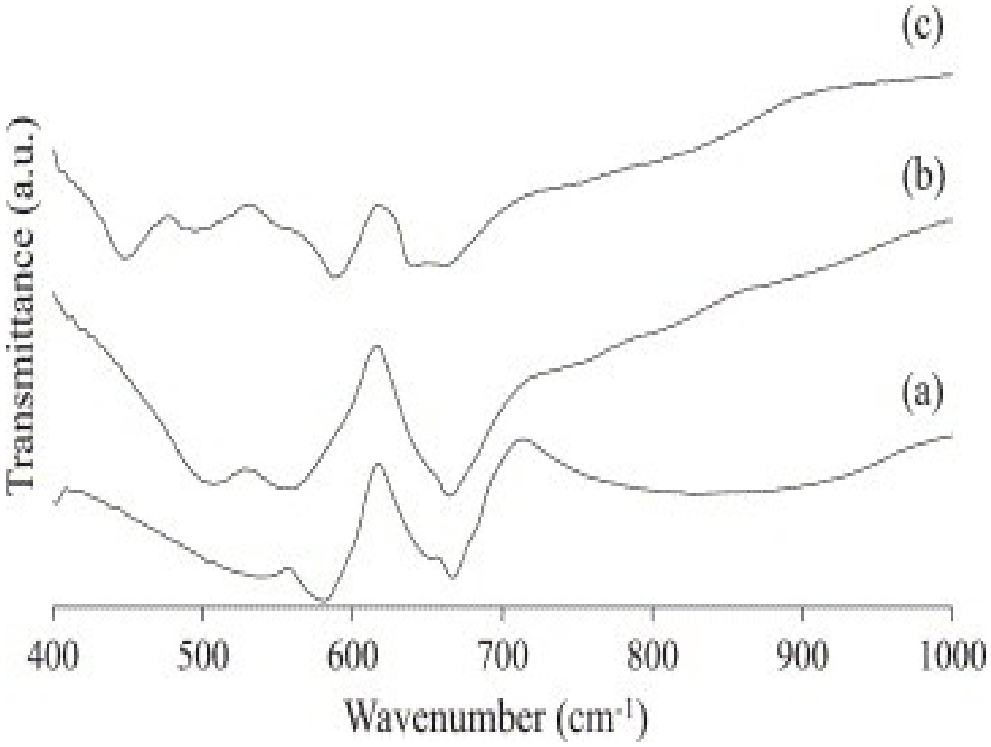

The XRD and FTIR analyses show that, when a mixture of Co_3O_4 at a rate of 180 °C h^{-1}, the formation of $CoAl_2O_4$ begins also below at 1000 °C, but it occurs more slowly than when a mixture of chlorides is submitted to the same thermal treatment. For the sample OX1200, the determination of the molar ratio Al/Co by EDS evidences also great heterogeneities of chemical composition, the ratio varying from 0.8 to 4.0.

4. Conclusion

The simultaneous reaction of cobalt chloride and aluminium chloride in molten $NaNO_3$–KNO_3 medium, at 450 °C for 2 h, does not lead directly to cobalt aluminate $CoAl_2O_4$, but to a mixture of crystallized cobalt oxide Co_3O_4 and amorphous γ-Al_2O_3, unlike for instance the synthesis of yttrium-stabilized zirconia. However, this intimate mixture exhibits a great reactivity since, on the one hand, the formation of $CoAl_2O_4$ is observed at a temperature as low as 800 °C when the mixture is heated at a rate of 180 °C h^{-1} and, on the other hand, the powder obtained at 1000 °C, without any dwell, is constituted of the spinel $CoAl_2O_4$ as major phase. Owing to its chemical composition homogeneity, morphological characteristics and localization of its absorption band, the powder appears suitable for its use as blue pigment.

If the same thermal treatment is applied to a mechanical mixture of either $CoCl_2$ and $AlCl_3$ or Co_3O_4 and γ-Al_2O_3, then $CoAl_2O_4$ represents only a minor phase. Moreover, the powders are much more heterogeneous in composition.

Acknowledgments

The authors would like to acknowledge Professor D.H. Kerridge for fruitful discussions about chemistry in molten salts and the Comité Mixte Interuniversitaire Franco-Marocain, which supports this work in the frame of the Action Integrée MA0368.

References

F. Singer, S. Singer, in Cerâmica Industrial, Vol. 1, ed. Urmo, S.A. de ediciones (Spane, Bilbao, 1976) p. 615.

G. Buxbaum, *Industrial Inorganic Pigments* (1st ed.), VCH, Weinheim, Germany (1993), p. 85.

L. Ji, S. Tang, H.C. Zeng, J. Lin and K.L. Tan, *Appl. Catal., A Gen.* **207** (2001), p. 247.

F. Bondioli, A.M. Ferrari, C. Leonelli and T. Manfredini, *Mater. Res. Bull.* **33** (1998), p. 723.

P.H. Bolt, F.H.P.M. Habraken and J.W. Geus, *J. Solid State Chem.* **135** (1998), p. 59.

S. Eric-Antonic, L. Kostic-Gvozdenovic, R. Dimitrijevic, S. Desportovic and L. Filipovic-Petrovic, *Key Eng. Mater.* **132–136** (1997), p. 30.

C. Otero Areán, M. Peòarroya Mentruit, E. Escalona Platero, F.X. LlabrésXamena, I. Xamena and J.B. Parra, *Mater. Lett.* **39** (1999), p. 22.

F. Meyer, R. Hempelmann, S. Mathur and M. Veith, *J. Mater. Chem.* **9** (1999), p. 1755.

S. Chemlal, A. Larbot, M. Persin, J. Sarrazin, M. Sghyar and M. Rafiq, *Mater. Res. Bull.* **35** (2000), p. 2515.

U.S. Strangar, B. Orel, M. Krajnc and R. Cerc. Korosec, *Mater. Technol.* **36** (2002), p. 6.

S. Chokkram, R. Srinivasan, D.R. Milburn and B.H. Davis, *J. Mol. Catal., A Chem.* **121** (1997), p. 157.

D.M.A. Melo, J.D. Cunha, J.D.G. Fernandes, M.I. Bernardi, M.A.F. Melo and A.E. Martinelli, *Mater. Res. Bull.* **38** (2003), p. 1559.

Z. Chen, E. Shi, W. Li, Y. Zheng and W. Zhong, *Mater. Lett.* **55** (2002), p. 281.

W.S. Cho and M. Kakihana, *J. Alloys Compd.* **287** (1999), p. 87.

M.I.B. Bernardi, S. Cava, C.O. Paiva-Santos, E.R. Leite, C.A. Paskocimas and E. Longo, *J. Eur. Ceram. Soc.* **22** (2002), p. 2911.

J. Merikhi, H.O. Jungk and C. Feldmann, *J. Mater. Chem.* **10** (2000), p. 1311.

D.H. Kerridge In: J.J. Lagowski, Editors, *The Chemistry of non aqueous solvents*, VB, New York (1978), p. 270.

B. Durand and M. Roubin, *Mat. Sci. Forum* **73–75** (1991), p. 663.

B. Durand, J.P. Deloume and M. Vrinat, *Mat. Sci. Forum* **152–153** (1994), p. 327.

H. Lux, *Z. Elektrochem.* **45** (1939), p. 303.

M. Descemond, M. Jebrouni, B. Durand, M. Roubin, C. Brodhag and F. Thevenot, *J. Mater. Sci.* **28** (1993), p. 3754.

D. Hamon, M. Vrinat, M. Breysse, B. Durand, L. Mosoni and T. des Courières, *Eur. J. Solid State Inorg.* **30** (1993), p. 713.

V. Harle, J.P. Deloume, L. Mosoni, B. Durand, M. Vrinat and M. Breysse, *Eur. J. Solid State Inorg.* **31** (1994), p. 197.

E. Kulikova, J.P. Deloume, B. Durand, L. Mosoni and M. Vrinat, *Eur. J. Solid State Inorg.* **31** (1994), p. 487.

A. Lakhlifi, C. Leroux, P. Satre, B. Durand, M. Roubin and G. Nihoul, *J. Solid State Chem.* **119** (1995), p. 289.

A. Aboujalil, J.P. Deloume, F. Chassagneux, J.P. Scharff and B. Durand, *J. Mater. Chem.* **8** (1998), p. 1601.

H. Frouzanfar and D.H. Kerridge, *Thermochim. Acta* **25** (1978), p. 11.

N.B. Singh and S.P. Pandey, *Thermochim. Acta* **67** (1983), p. 147.

L.E. Topol, R.A. Osteryoung and J.H. Christie, *J. Phys. Chem.* **70** (1966), p. 2857.

D.H. Kerridge and W.M. Shakir, *Thermochim. Acta* **182** (1991), p. 107.

A. Gadsden Aric, *Infrared Spectra of Minerals and Related Inorganic Compounds* (1975), p. 44.

M.I. Baraton and P. Quintard, *J. Mol. Struct.* **79** (1982), p. 337.

Corresponding author. Tel.: +33 05 61 55 61 40; fax: +33 05 61 55 61 63.

Original text : Elsevier.com